Functionalization of silicon nanowires for specific sensing

V. Passi, Emmanuel Dubois, C. Celle, S. Clavaguera, J.P. Simonato, J.P. Raskin

Functionalization of Silicon Nanowires for Specific Sensing

V. Passi[a], E. Dubois[b], C. Celle[c], S. Clavaguera[c], J.-P. Simonato[c], J.-P. Raskin[a]

[a] Institute of Information and Communication Technologies, Electronics and Applied Mathematics, Université catholique de Louvain, 1348 Louvain-la-Neuve, Belgium
[b] Institut d'Electronique, de Microelectronique et de Nanotechnology (IEMN), Silicon Microelectronics Group, Cité Scientific, Avenue Poincaré, BP 60069, F-59652, Villeneuve d'Ascq Cedex, France
[c] CEA–Grenoble, LITEN/DTNM/LCRE, 17 Rue des Martyrs, 28054 Grenoble Cedex 9, France

Thanks to their large surface-to-volume ratio, silicon nanowires (Si NWs) are extremely sensitive to all phenomena which could alter their surface potential and charge distribution. Those surface variations lead to a change of the Si NWs equivalent conductance. The use of the output conductance of a silicon nanowire as a compact transducer for direct detection of (bio)chemical molecules or gases has gained immense attention these last years. In this paper, fabrication of silicon nanowires using top-down approach is shown, with simple calculations to determine hole mobility, hole concentration and resistivity. Transfer characteristics and sampling measurements were performed on the nanowires with and without surface functionalization under various ambient conditions indicating the importance of functionalization in order to avoid any environment effect on the transport properties of the nanowires.

Introduction

Owing to different properties when compared to the bulk material, unique applications in all fields, silicon nanowires have now become a subject of immense study. It is well acknowledged that one dimensional (1-D) silicon nanowires are excellent systems to investigate the dependence of electrical transport and chemical properties. Silicon nanowires (Si NWs) are of exceptional interest because their surface can be modified to act as both interconnect (1) (2) and functional units such as immobilizing matrices in fabricating electronic, electrochemical devices (3) (4) (5) (6) with nanoscale dimensions. Due to large surface-to-volume ratio and quasi 1-D characteristics, Si NWs can be used as ultra high sensitivity sensors for DNA detection (7) (8) (9). However, Si NWs themselves have no chemical specificity and in order to detect certain target species the surface of the Si NWs has to be functionalized with molecules that can interact with the specific target species which are to be detected. The sensing mechanism is related to: (i) change in density of silicon surface states, (ii) creation of a net charge in the molecules which act as an effective top-gate, or (iii) charge transfer between silicon and the functionalized molecules (10) (11) (12) (13). Selective functionalization of Si NW array is important since it improves the sensitivity, selectivity and detection limit of the sensor while keeping the surrounding areas inert. In this paper, we report the fabrication of silicon nanowires of various widths and lengths, using top-down approach and graft the surface of the wires using either (i) 3-(4-ethynylbenzyl)-1, 5, 7-trimethyl-3-azabicyclo

[3.3.1] nonane-7-methanol (EBTAM), or (ii) OctadecylTrichloroSilane (OTS). Electrical measurements were carried out on the nanowires before and after functionalization with these molecules and reduction of hysteresis are observed on functionalized wires.

Fabrication

Single crystalline Silicon nanowires of various dimensions are fabricated using top-down approach using electron beam lithography and reactive ion etching. The fabrication process is presented in an earlier work (14). In brief, starting with a silicon-on-insulator wafer, hydrogen silsesquioxane (HSQ) - a negative tone electron beam (e-beam) resist - is spin-coated. Followed with electron beam exposure the resist is developed in tetramethylammonium hydroxide solution (TMAH-25%). Figure 1a shows the nanowires after development of HSQ. Using Chlorine chemistry and HSQ as an etch mask, top-silicon is etched to define nanowires along with large pads in silicon. HSQ is removed by immersing the wafer in HF-1% for 30 s as shown in Fig. 1b. Then, PMMA is spin-coated followed by exposure of patterns in order to open windows to deposit metal (Fig. 1c). After the development of the resist and the dip of the wafer in HF-1% in order to remove native oxide, platinum is deposited to a thickness of 20 nm. Excess platinum is removed by lift-off in acetone. After inspecting the wafer with scanning electron microscope (SEM) (Fig. 1d), annealing of the metal is completed. Array of 10 nanowires of width of 25, 50, 75, and 100 nm, with length of 0.3, 0.6, 1.2 and 2.4 µm and spacing of 0.3 µm, and 1 nanoribbon (shown as the inset of Fig. 1d) of width 1 µm, length 10 µm are fabricated on the same wafer, functionalized and measured.

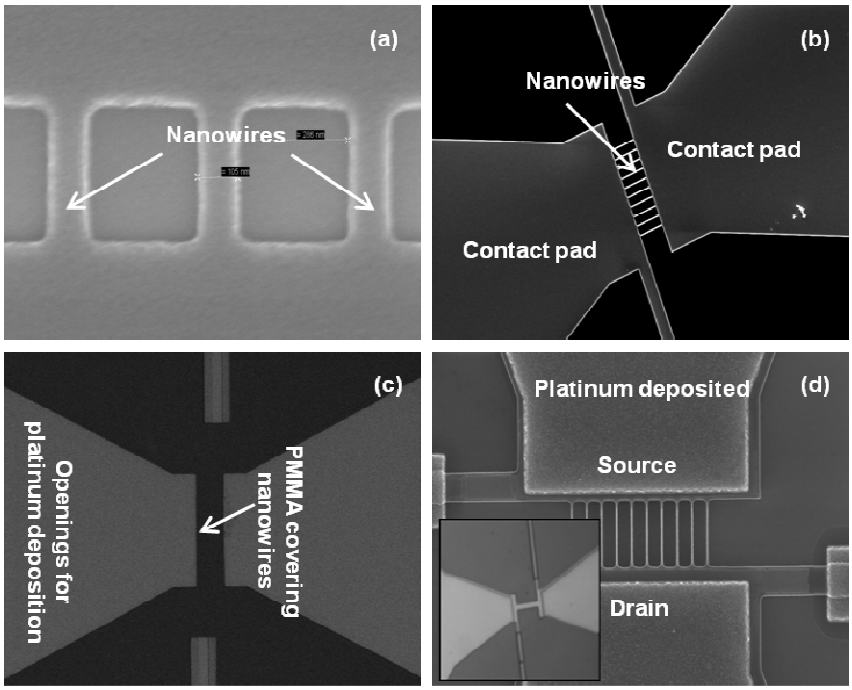

Figure 1. Top-view SEM image of silicon nanowires at various stages of the fabrication. (a) After resist development, (b) after top-silicon etching and HSQ removal, (c) after exposure of PMMA to make windows for metal deposition, and (d) after lift-off of platinum on the source and drain pads. The inset of Fig. 1d shows the fabricated single microwire: width = 1 µm and length = 10 µm.

Electrical Measurements

Electrical characterization of the nanowires before and after functionalization is performed using B1500 Agilent semiconductor device analyzer. Figure 2 shows the transfer characteristics of an array of 10 nanowires of width 25 nm and length 300 nm, measured in ambient air at fixed drain-source voltage (V_{ds}) of 2 V. The backgate bias is varied from +20 V to -20 V in step of 1 V with a hold and delay time of 0.5 s and 0.2 s, respectively. The value of transconductance can be determined by fitting the linear part of the graph. The values of transconductance (G_m) and turn-on threshold voltage (V_{th}) are 1080 nS and 12 V, respectively (extracted from Fig. 2b). A simple calculation to determine the resistivity is shown below.

The capacitance, hole mobility, hole concentration and resistivity are calculated using the equations [1]-[4] (15), respectively, as given below.

$$C = n\,\varepsilon_0\,\varepsilon_{SiO2}\,L_{nw}\,W_{nw} / T_{box} \quad [1]$$

$$G_m = \delta I_{ds} / \delta V_{bg} = \mu_{hole}\,C\,V_{ds} / L_{nw}^2 \quad [2]$$

$$n_{hole} = V_{th}\,C / (n\,q\,W_{nw}\,T_{nw}\,L_{nw}) \quad [3]$$

$$\rho = 1 / n_{hole}\,q\,\mu_{hole} \quad [4]$$

Where C is the capacitance in Farad, n is the number of wires (10 in our case), ε_0 is the permittivity of free space (8.854×10^{-12} F/m), ε_{SiO2} is the dielectric constant of silicon-dioxide (3.9), L_{nw} is the length of the nanowire (300 nm), T_{box} is the thickness of buried-oxide (400 nm), W_{nw} is the width of the silicon nanowire, V_{ds} = 2 V, T_{nw} is the thickness of top-silicon/nanowire (50 nm). The values for capacitance, hole mobility, hole concentration and resistivity are 6.47×10^{-18} F, 75.1 cm² / V.s, 1.27×10^{17} / cm³, 0.64 Ω-cm, respectively.

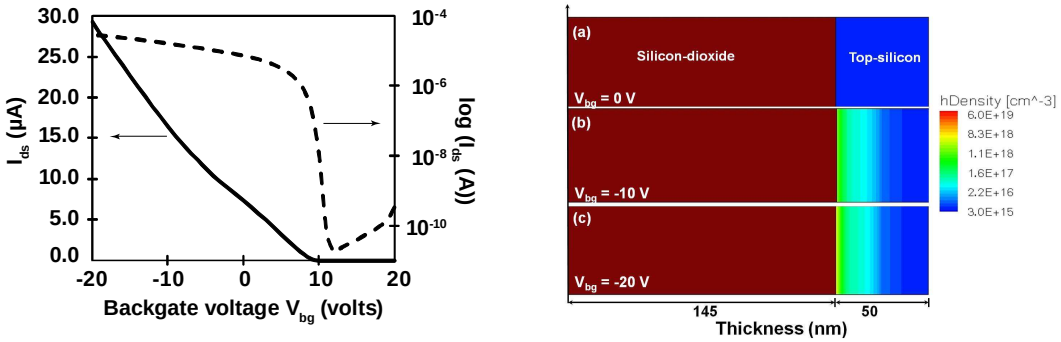

Figure 2. (a) Transfer characteristics (I_{ds}-V_{bg}) of an array of nanowires of width 25 nm and length 300 nm measured in ambient air. Solid line is linear scale on the left hand side and the dotted line is the log scale on the right hand side, respectively. (b) 2-D simulations (without considering the traps at interfaces) showing the hole density in top-silicon of thickness 50 nm for three different backgate bias values for V_{ds} = 0.1 V.

The value of hole mobility obtained from the measurement is much lower than expected bulk mobility since the carrier transport is mainly in the thin surface layer (surface

mobility) rather than in the core of the wires. The increase in scattering centers (created due to reactive-ion-etching of the top-silicon to define the nanowires), also accounts to the reduction of carrier transport in the nanowires. The resistivity is 20 times lower than the original unintentionally doped SOI wafers. Figure 2b shows the hole concentration in the nanowires for various backgate voltages (0 V, -10 V, and -20 V) for fixed V_{ds} = 0.1 V. The top-silicon is depleted for V_{bg} = 0 V and for negative V_{bg} the top-silicon is accumulated with holes which are closer to the buried-oxide and bulk-silicon interface.

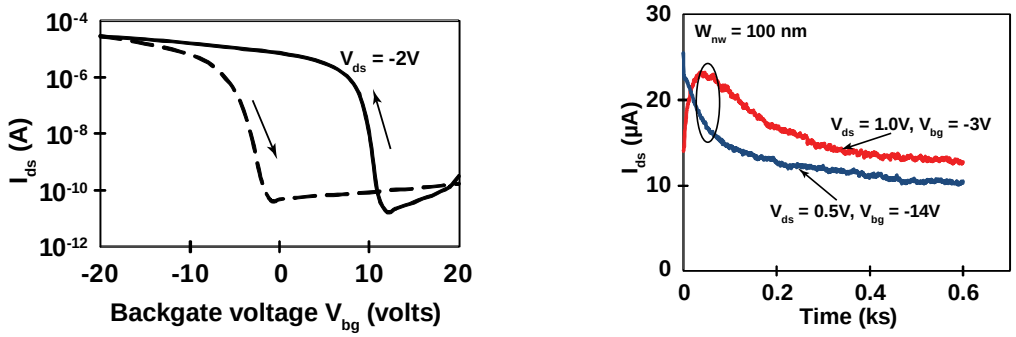

(a) (b)

Figure 3. (a) Transfer characteristics (I_{ds}-V_{bg}) of an array of nanowires of width 100 nm and length 300 nm measured in ambient air. Solid black line is forward sweep from +20 V to -20 V and the dotted black line is reverse sweep, respectively. (b) Sampling measurements showing the current variation with time under various backgate biases.

Hysteresis is observed as can be seen from Figure 3a, when the measurements are carried out in ambient air on nanowires without any functionalization. Figure 3b represents sampling measurements for a 50 nm-thick top-silicon thickness, (an array of 10 nanowires) 100 nm-wide and 300 nm-long for two different backgate voltages (-3 V and -14 V) in ambient air. Not even after 10 minutes of measurement a steady state is reached. In order to understand the hysteresis effect measurements were performed in dry air and under vacuum (~80 mTorr). Figures 4a-4c show the I_{ds}-V_{bg} measurements on nanowires under ambient air, dry air and vacuum, respectively. Reduction of hysteresis is observed when measurements are performed in dry air and vacuum. The hysteresis of the nanowires depends on the environment; however, this can be missed since it takes relatively long time for appreciable effects to take place (16). By changing the environment from ambient air to dry air, noticeable decrease in hysteresis is observed (Figure 4a versus Figure 4b). By measuring the nanowires under vacuum (~80 mTorr) further reduction in hysteresis is observed but does not vanish completely indicating that the vacuum level is not sufficient. The causes of hysteresis could be the charge trapping by water molecules on the surface of the nanowires when exposed to ambient air. There are two possible types of charge traps, (i) water molecules which are weakly adsorbed on the nanowire surface, which can be easily removed by pumping in vacuum, (ii) silicon-dioxide surface bound water in close proximity to the nanowires. Silicon surface consists of Si-OH silanol groups which are hydrated by water molecules that are hydrogen bonded to the silanol (17) (18) (19). It is well known that hydrophilic silicon surface contains adsorbed water layer in atmospheric conditions and at temperature below 200°C (20), and a monolayer or sub-monolayer of hydrogen-bonded water remains on the silicon-dioxide and cannot be removed by pumping in vacuum (17) (18) (19). This water is known to act

as a slow charge traps in conventional MOS devices (21) (22) (23), which leads to the conclusion that surface water is largely responsible for the hysteresis in the nanowires.

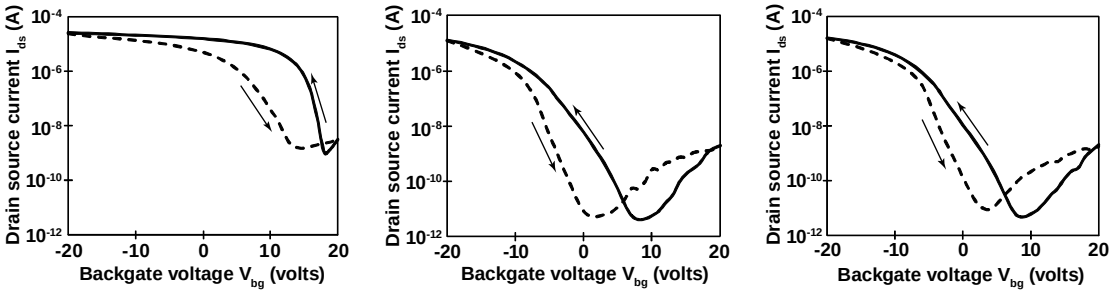

(a) (b) (c)

Figure 4: Transfer characteristics of nanowires under various environment conditions: (a) ambient air, (b) dry air and (c) vacuum. Solid lines represent forward (+20 V to -20 V) and dashed lines represent backward sweep (-20 V to +20 V) respectively.

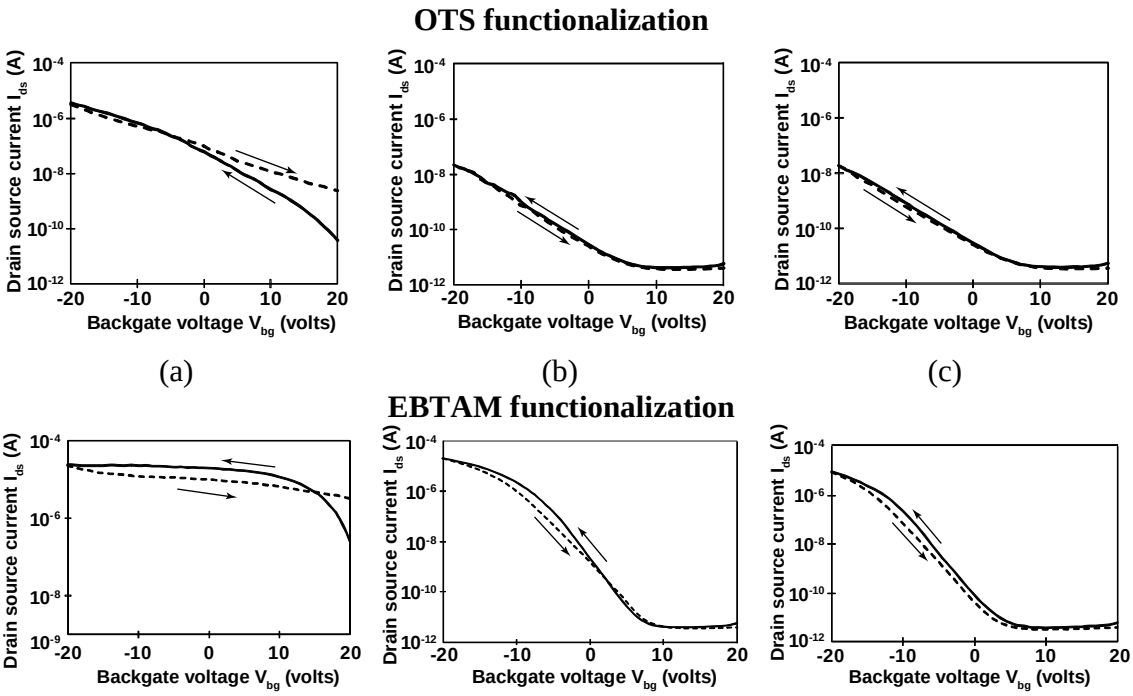

(a) (b) (c)

(e) (f) (g)

Figure 5. Transfer characteristics of functionalized nanowires under various environment conditions: (a, d) ambient air, (b, e) dry air and (c, f) vacuum.

In order to avoid any environmental effect on the transport in nanowires (the hysteresis and current variation with time) functionalization of the nanowires with either (i) EBTAM or (ii) OTS was carried out. Grafting of EBTAM was done on hydrogen terminated silicon surface obtained by short HF dip whereas OTS molecules are grafted onto native oxide formed on the nanowire surface (24). Figures 5a-5c show the transfer characteristics of nanowires and nanoribbons after functionalization with OTS. Drastic reduction of hysteresis is observed after grafting with either of the molecules indicating the reduction of adsorbed water molecules on the surface of the nanowires (25). The above results clearly show the impact of surface states/charges which are predominant at

the nanoscale. Understanding the effect of surface states/ions on the transport properties at the nanoscale is not straight forward but in order to do so it is evident that surface states must be well controlled to avoid any misleading or incorrect interpretation of the results.

Conclusion

Single crystalline silicon nanowires were fabricated using top-down approach and transport properties of these nanowires were studied. It was found that the resistivity of the nanowires is lower than the original wafer. The conductivity of the nanowires exhibits very high sensitivity to humidity. Surface modification with EBTAM and OTS make the nanowires immune to the surroundings. These functionalized nanowires can be used as gas sensors. Transfer characteristics demonstrate that surface states dominate the transport properties, and surface passivation can improve the device performance and reliability.

References

1. V. Jousseaume, V. T. Renard, *Interconnect Technology Conference*, pp. 1-3, 2010.
2. A. D. Wissner-Gross, *Institute of Physics Publishing, Nanotechnology*, pp. 4896-4990, 2006.
3. A. K. Wanekaya *et al*., *Electroanalysis* 18, pp. 533-550, 2006.
4. R. E. Chee, *et al*., *ICBME Proceedings*, 23, pp. 838-841, 2009.
5. M.-W. Shao, *et al*., *Journal of Chem. Sci.*, vol. 121, no. 3, pp. 323-327, 2009.
6. L. Mai, *et al*., *Nano Letters*, vol. 10, pp. 4273-4278, 2010.
7. G.-J. Zhang, *et al*., *Nano Letters*, vol. 8, no. 4, pp. 1066-1070, 2008.
8. C.-H. Lin, *et al*., *Biosensors and Bioelecronics*, vol. 24, pp. 3019-3024, 2009.
9. J.-I. Hahm, C.M. Lieber, *Nano Letters*, vol. 4, no. 1, pp. 51-54, 2004.
10. D. Cahen, *et al*., *Advanced Functional Materials*, vol. 15, pp. 1571-1578, 2005.
11. O. Shaya, *et al*., *Applied Physics Letters*, vol. 93, 043509, 2008.
12. N. Elfstrom, *et al*., *Nano Letters*, vol. 7, pp. 2606-2612, 2007.
13. R. Cohen, *et al*., *Journal of Am. Chemical Society*, vol. 121, pp. 10545-10553, 1999.
14. V. Passi, *et al*., *The 23rd IEEE Intl. Conf. on Micro Electro Mechanical Systems MEMS 2010*, Hong Kong, pp. 464-467, 2009.
15. G. D. Yuan, *et al*., *ACS Nano*, vol. 4, no.6, pp. 3045-3052, 2010.
16. W. Kim, *et al*., *Nano Letters*, vol. 3, no. 2, pp. 193-198, 2003.
17. N. Tas, *et al*., *J. Micromech. Microeng*., vol. 6, pp. 385-397, 1996.
18. R. K. Iler, "The chemistry of silica: Solubility, polymerization, colloid and surface properties and biochemistry", Wiley - New York, 1979.
19. M. L. Hair, "Infrared spectroscopy in surface chemistry", Marcel Dekker - New York, 1967.
20. L. T. Zhuravlev, *Colloids and Surface A: Physicochemical and Engineering Aspects*, vol. 173, issues 1-3, pp. 1-38, 2000.
21. M. O. Andersson, *et al*., *Journal of Applied Physics*, vol. 71, pp. 846-1852, 1992.
22. J. F. Zhang, B. Eccleston, *IEEE Trans. Electron Devices*, vol. 41, pp. 740-744, 1994.
23. J. S. Chou, S. C. Lee, *IEEE Trans. Electron Devices*, vol. 43, pp. 599-604, 1996.
24. D. K. Aswal, *et al*., *Analytica Chimica Acta*, vol. 568, pp. 84-108, 2006.
25. D. Wang, *et al*., *J. AM. Chem. Soc*, pp. 11602-11611, 2004.